Influence of oxygen pressure on the ferroelectric properties of epitaxial $BiFeO_3$ thin films by pulsed laser deposition

Lu You,[1] Ngeah Theng Chua,[1] Kui Yao,[2] Lang Chen,[1] and Junling Wang[1,*]
[1]*School of Materials Science and Engineering, Nanyang Technological University, Singapore 639798, Singapore*
[2]*Institute of Materials Research and Engineering, A*STAR (Agency for Science, Technology and Research), 3 Research Link, Singapore 117602, Singapore*

(Received 5 April 2009; revised manuscript received 15 June 2009; published 7 July 2009)

The growth window of multiferroic $BiFeO_3$ thin films is very small. Both temperature and oxygen pressure will affect the film quality and phase purity significantly. We demonstrate here that even within the window where phase pure $BiFeO_3$ thin films can be obtained, different oxygen partial pressures still lead to substantial variation in Bi/Fe ratio in the film, which closely link with the corresponding ferroelectric properties. Piezoelectric force microscopy also reveals significant difference in the domain structures of these films. A defect-dipole complex model is proposed to explain the difference in the electrical properties and domain structures for films grown under different oxygen pressures.

DOI: 10.1103/PhysRevB.80.024105 PACS number(s): 77.84.−s, 77.80.Dj

I. INTRODUCTION

Multiferroic $BiFeO_3$ (BFO) has attracted considerable attention since the day its intrinsic large polarization was confirmed in the thin-film form.[1] Although the magnetic response of BFO thin films is controversial,[2,3] to date BFO is still the only known single-phase material with both robust ferroelectric (Curie temperature ~820 °C) (Ref. 4) and magnetic (Neél temperature ~370 °C) (Ref. 5) orderings coexisting at room temperature. Furthermore, the direct coupling between these order parameters[6,7] makes electrical control of magnetism possible, which paves the way for bridging the electronic and spintronic industries.[8]

Bulk BFO has a highly distorted perovskite structure with rhombohedral symmetry.[9] The large relative displacement between Bi and O is believed to originate from the high stereochemical activity of Bi lone pair,[10] giving rise to a large spontaneous polarization ~100 $\mu C/cm^2$ along the pseudocubic $(111)_{pc}$ direction,[11] which makes it a potential lead-free substitute for traditional lead zirconium titanate (PZT). However, the growth window of phase pure BFO thin film is very small. Bi_2O_3 and Fe_2O_3 are the two typical impurities.[12,13] The former usually results in large leakage current of the films, while the latter causes artifacts in magnetic measurements. Recently, Bea *et al.*[14] explored the influence of growth temperature and oxygen pressure on BFO thin films, thus mapping out the pressure-temperature phase diagram for BFO deposition. According to their results, low-temperature/high-oxygen-pressure condition results in excess Bi while the opposite condition leads to iron oxide formation. Consistent with their result, we found similar trend in Bi/Fe ratio with respect to the growth pressure using a stoichiometric target. Furthermore, even though single-phase BFO films could be obtained within certain oxygen pressure range, their properties vary dramatically as deposition pressure changes within the range.

In this paper, the Bi/Fe ratio of BFO films grown under different oxygen pressures and the corresponding electrical properties were investigated. It was found that the ferroelectric properties and domain structure were closely related to the Bi/Fe ratio. A defect-dipole complex model was proposed to explain the observed experimental results.

II. EXPERIMENTAL PROCEDURE

Epitaxial BFO films were deposited on $SrRuO_3$ coated $SrTiO_3$ $(100)_c$ single-crystal substrates by pulsed laser deposition. A stoichiometric target was ablated by using a KrF excimer laser (λ=248 nm) with an energy density of ~1 J/cm^2 and a repetition rate of 10 Hz. The growth temperature was fixed at 700 °C, while the oxygen partial pressure was varied between 1 and 100 mTorr. All films had a thickness around 200 nm determined by a step profiler. The structure and crystalline quality of the films were studied using a high-resolution x-ray diffractometer (XRD) (Panalytical X-pert Pro). Chemical analyses were performed by energy dispersive x-ray spectroscopy (EDS) equipped on a JSM-6360 scanning electron microscope. Square Pt top electrodes of 40 μm were prepared via a standard photolithography process for electrical measurements. Ferroelectric and dielectric properties were measured by Precision *LC* ferroelectric tester (Radiant Technologies) and Agilent E4980A Precision *LCR* meter, respectively. Piezoresponse force microscopy and local piezoelectric hysteresis loop measurements were carried out on an atomic force microscope (Asylum Research MFP-3D) using Pt/Ir-coated tips. Magnetic properties of the thin films were studied by vibrating sample magnetometer (LakeShore 7400) at room temperature.

III. RESULTS AND DISCUSSION

Figure 1 shows the XRD patterns of films grown under different oxygen pressures. Phase pure BFO films can be obtained within a relative broad pressure range of 1–20 mTorr at 700 °C. Within this range, no Fe_2O_3 phase is observed within the detection limit. However, once oxygen pressure goes above 20 mTorr, extra peaks that can be attributed to Bi_2O_3 appear. Note that a stoichiometric target is used in this study, which explains the slightly different deposition window from Ref. 14. It also demonstrates that the

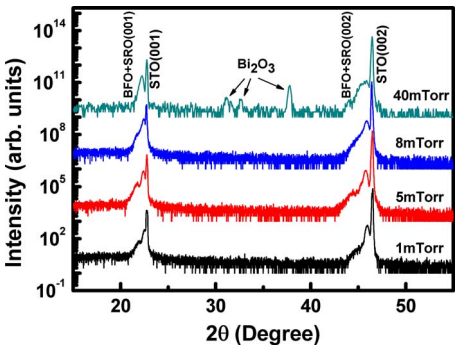

FIG. 1. (Color online) XRD patterns of BFO epitaxial films grown under different oxygen pressures. Peaks of Bi_2O_3 second phase are indicated by arrows.

film composition can be controlled by varying the deposition parameters without using Bi-excess targets. The calculated out-of-plane lattice constants of films deposited at 1, 5, 8, and 40 mTorr are 3.952, 3.974, 3.972, and 3.995 Å, respectively, increasing with the oxygen pressure. The intensities of the BFO peaks also increase, indicating improved crystallinity.

The ferroelectric hysteresis loop at 1 kHz and leakage behavior of films grown under different oxygen pressures are shown in Figs. 2(a) and 2(b). As the deposition pressure decreases, the remanent polarization continues to drop and the hysteresis loop becomes more canting. No significant change in the coercive field is observed. However, there is minor imprint effect for low-pressure samples, corresponding to a preferred polarization "up" state. Accompanying the change in polarization, the films grown under low oxygen pressure show similar leakage current while those grown under 20 mTorr or higher show leakage current density about two to three orders of magnitude larger. The dielectric and piezoelectric coefficient d_{33} hysteresis loops were measured using 50 kHz ac oscillations with amplitudes of 100 mV and 1 V, respectively, superimposed on a dc bias. The results were plotted in Figs. 2(c) and 2(d), both showing similar decreasing trend as the pressure goes down. The data for films grown under high oxygen pressure could not be acquired because their low resistivities led to electrical breakdown during dc bias sweep. All the samples grown under low oxygen pressure show a clear loop shift consistent with the polarization hysteresis loop. Besides, the dielectric *C-V* curves show obvious double-loop feature with two peaks appearing at the coercive field and around zero bias.

In order to unravel the variations in the electrical properties of BFO films deposited under different oxygen pressures, compositional analyses were carried out by EDS. A standard stoichiometric BFO target was used for calibration. For each sample, the measurement was performed by mapping certain area at different locations of the film. The results are self-consistent within each film and are plotted in Fig. 3. It is clear that the Bi/Fe ratio in the films decreases as deposition pressure decreases [Fig. 3(a)]. Surprisingly, the Bi/Fe ratio can go down to as low as ~0.6 without Fe_2O_3 formation according to the XRD pattern, while a small Bi excess will give rise to Bi_2O_3 phases. The decrease in Bi/Fe ratio with reduced oxygen pressure is consistent with the decrease in the out-of-plane lattice constant and the crystallinity of the films. Magnetic properties were also measured to confirm the absence of magnetic Fe_2O_3 phases (not shown). All the films exhibited weak magnetizations below $0.06\mu_B$/Fe, showing no trace of magnetic Fe_2O_3 existence. The large bismuth deficiencies indicate broad single-phase field in the Bi-poor region. This agrees with the previous report[15] and is similar to the $PbTiO_3$ system.[16]

The remanent polarization P_r derived from positive-up–negative-down pulse measurement, relative permittivity ε_r, and resistivity all show direct correlation with the Bi/Fe ratio as depicted in Fig. 3(b). As we know, Bi displacement contributes significantly to the spontaneous polarization of BFO. So it is not surprising that the polarization will decrease

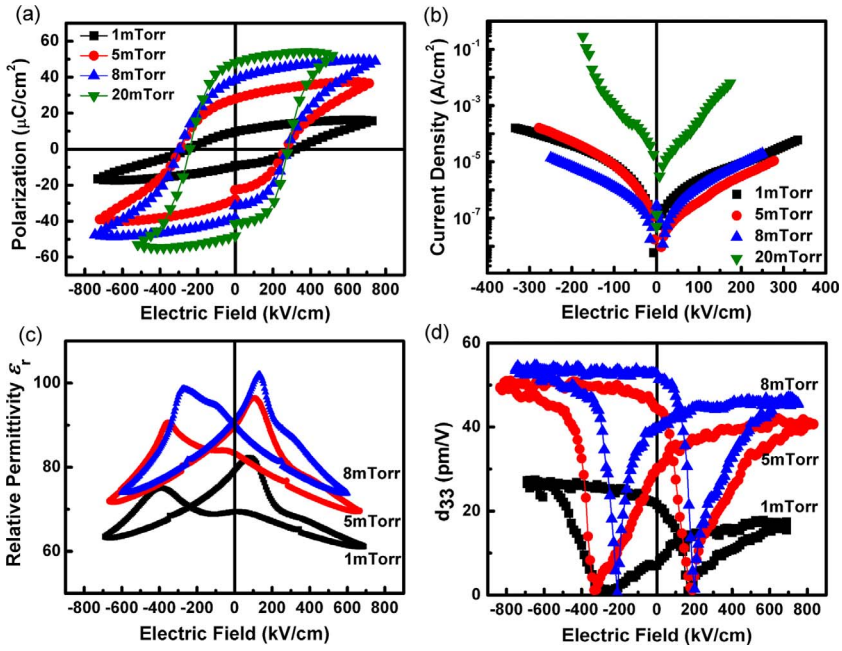

FIG. 2. (Color online) (a) Ferroelectric polarization, (b) leakage current density, (c) relative permittivity, and (d) piezoelectric coefficient d_{33} as a function of electric field for BFO films deposited under different oxygen pressures.

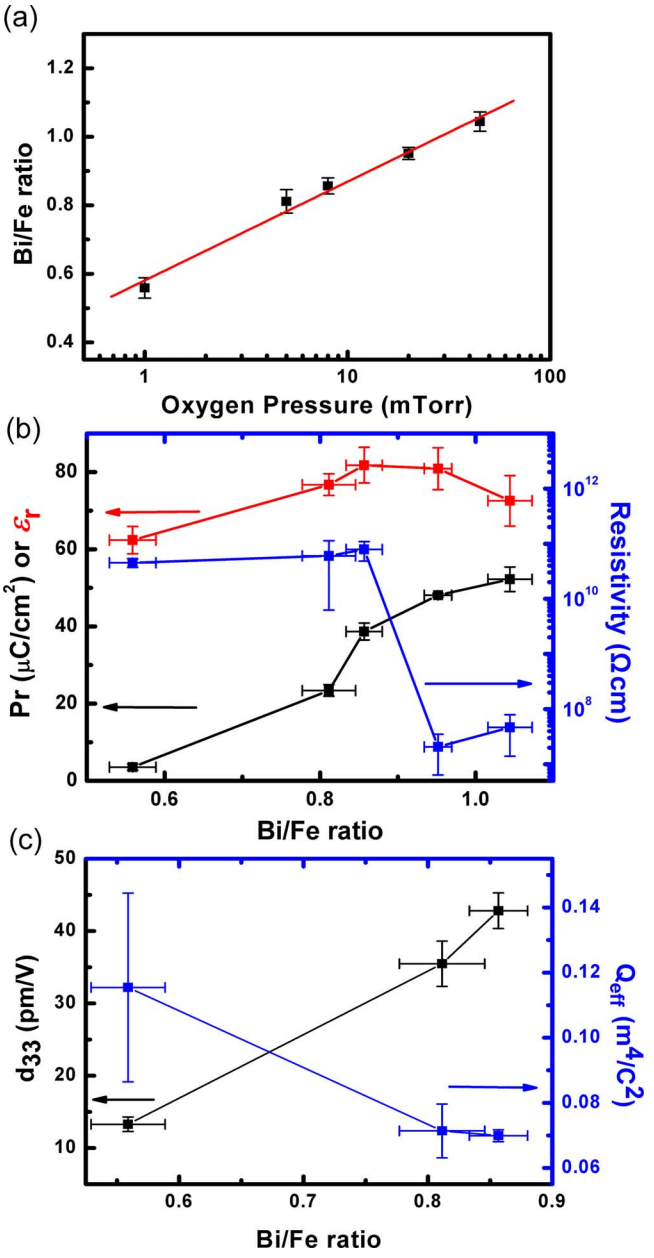

FIG. 3. (Color online) (a) Plot of Bi/Fe ratio as a function of deposition oxygen pressure, (b) plot of remanent polarization, relative permittivity, and resistivity at 100 kV/cm as a function of Bi/Fe ratio, and (c) plot of remanent d_{33} and electrostrictive coefficient Q_{eff} as a function of Bi/Fe ratio for different BFO thin-film samples. The red line in (a) is to guide the eyes.

when more Bi vacancies (V''_{Bi}) are introduced. The gradual canting of the ferroelectric hysteresis loop with the decease in Bi concentration is also a reminiscence of ferroelectric fatigue which is claimed to result from domain pinning by defects.[17] Oxygen vacancies ($V_{\text{O}}^{\cdot\cdot}$) are widely reported point defects in ferroelectric thin films.[18] Positively charged $V_{\text{O}}^{\cdot\cdot}$ can combine with negatively charged V''_{Bi} to form defect-dipole complexes which are effective in ferroelectric domain pinning.[19,20] This could also be a reason for the reduced polarization in Bi-poor region. When the composition enters into the Bi-excess range, however, the polarization remains almost constant as deposition pressure increases, confirming the intrinsic polarization of BFO to be ~55 $\mu\text{C}/\text{cm}^2$ along $(001)_{\text{pc}}$.

In contrast, the resistivity shows reverse trend with respect to the Bi/Fe ratio. Large leakage current in BFO thin films is widely reported, which is mainly due to the oxygen vacancies or conductive Bi_2O_3 phases rather than the intrinsic property of BFO.[21] The Bi deficiency reported here can be considered as Bi vacancy doping, which will greatly compensate the oxygen vacancies and obviously eliminate the presence of Bi_2O_3. As a result, the leakage currents in Bi-deficient samples are much smaller than those stoichiometric or Bi-rich ones [Fig. 2(b)]. In this sense, introducing Bi vacancies is equivalent to the widely adapted altervalent/aliovalent cation doping,[22–25] providing a way for tuning electrical properties of BFO thin films.

The relative permittivity shows less dependence on the Bi content with values around 60–80. Frequency-dependence dielectric spectroscopy (not shown) indicates only small dielectric relaxation up to 2 MHz, which confirms the intrinsic contribution. According to the semiempirical phenomenological equation, the piezoelectric coefficient in a single crystal can be expressed as a function of intrinsic relative permittivity ε_{int}, polarization P, and electrostrictive coefficient Q,[26]

$$d_{33} = 2\varepsilon_0\varepsilon_{\text{int}}Q_{\text{eff}}P, \tag{1}$$

where ε_0 is the vacuum permittivity and Q_{eff} is effective electrostrictive coefficient along [001] direction. The measured remanent d_{33} and calculated Q_{eff} are plotted against the Bi/Fe ratio shown in Fig. 3(c). The calculated Q_{eff} ~0.07 m^4/C^2 for more stoichiometric samples is close to the Q_{11} of PZT thin films[26] but deviated from previous report.[27]

Piezoelectric force microscopy was performed to study the domain structures and local piezoelectric response. Pt/Ir-coated highly doped Si tips (spring constant of ~42 N/m, resonance frequency of ~320 kHz, and tip radius of ~25 nm) were used. The scans were performed under ambient condition, with a 50 kHz ac voltage of 6 V peak to peak applied to the tip. Yellow (bright) and purple (dark) contrasts in Fig. 4 represent polarization component pointing "up" and "down," respectively. Films grown under low oxygen partial pressure (5 mTorr) show topographic features consistent with island growth mode [Fig. 4(a)]. As shown in Fig. 4(c), the ferroelectric domains exhibit a fractal characteristic with average domain size of ~50 nm, similar to those studied in thin BFO films.[28] Local d_{33} hysteresis loop [Fig. 4(e)] reveals a slight shift of the hysteresis loop toward negative bias, consistent with the dominating preferred polarization direction in the image. As deposition pressure increases to 20 mTorr, drastically different topographic features are observed [Fig. 4(b)] possibly due to a change to step flow growth mode. Large domains of micron size are observed. Grain-boundary-like trenches are formed likely to reduce the mismatch of elastic distortions between individual domains. The domain boundaries could be another source of high leakage current.[29] Within each domain, preferred polarization in up or down direction is observed [Fig. 4(d)]. Local d_{33} hyster-

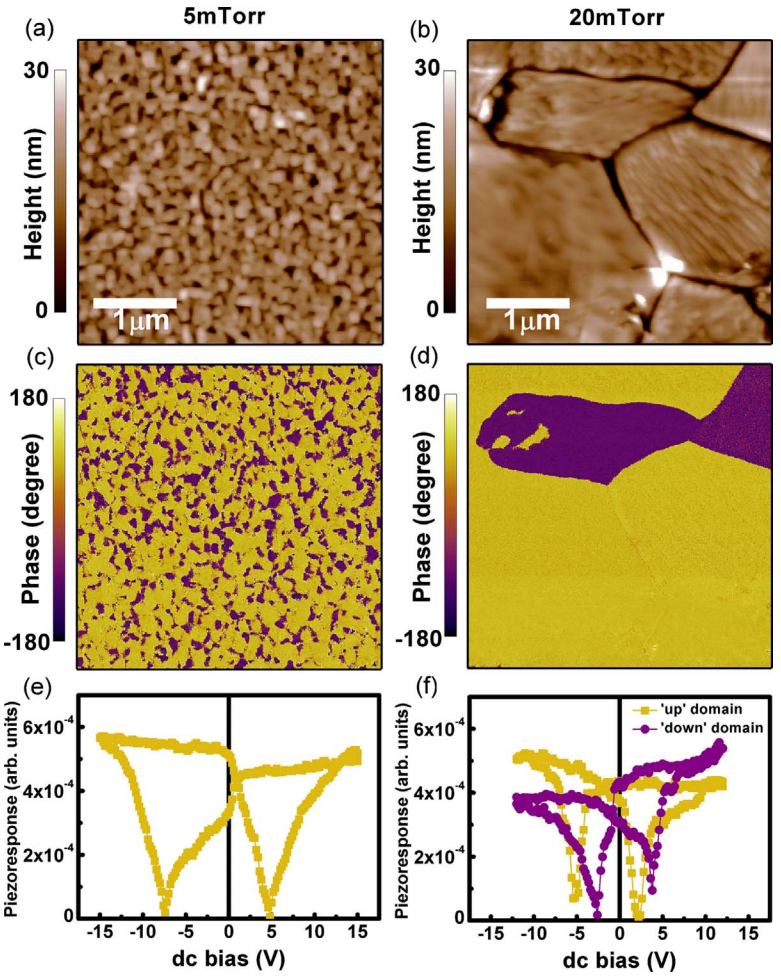

FIG. 4. (Color online) (a) and (b) 3×3 μm^2 topographic images; (c) and (d) corresponding piezoresponse phase images and (e) and (f) local d_{33} hysteresis loops of BFO films grown under 5 and 20 mTorr oxygen pressures. The scales in (a) and (b) and (c) and (d) are 30 nm and 360°, respectively. Yellow (bright) and purple (dark) loops in (f) represent original up and down domains, respectively.

esis loop measurements reveal opposite imprint behaviors, consistent with the preferred polarization direction.

To what extent does the growth mode affect the ferroelectric domain structure is unknown currently. But we suggest that defects in the films also play an important role. For films grown under low oxygen pressure, high-concentration Bi vacancies and oxygen vacancies may form V''_{Bi}-$V^{\cdot\cdot}_{O}$ defect-dipole complexes. Such defect-dipole complexes will produce an internal field, leading to a preferred direction of the ferroelectric domain. Due to the randomly located nature of the defect-dipole complexes, the polarization is also randomly oriented up and down. For films grown under high oxygen pressure, large domains can form due to the lack of such defect-dipole complexes. This model also explains the double peaks of dielectric response as depicted in Fig. 5. Under a large dc field, all the domains can be poled in one direction. However, the defect dipoles are unable or very difficult to be reoriented by external field due to their immobile nature. After removal of the external field or by applying a small field with opposite polarity, part of the ferroelectric domains will reverse with the assistance of the internal field, giving rise to a peak close to the zero bias in *C*-*V* curve. The difference in the peak amplitude is consistent with the relative fractions of up and down domains in the original state [Fig. 4(c)].

IV. CONCLUSIONS

In summary, we have studied the effect of oxygen pressure on the electrical properties of BFO thin films. Even within the deposition window where phase pure films can be obtained, it is observed that Bi/Fe ratio in the films decreases

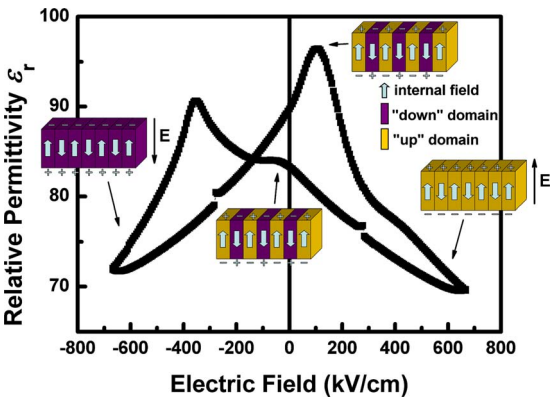

FIG. 5. (Color online) Dielectric hysteresis loop of 5 mTorr BFO thin film with ferroelectric domain configuration at different stages. The light blue (bright) arrows indicate internal field induced by defect-dipole complexes. Yellow (bright) and purple (dark) domains represent up and down domains, respectively.

with the deposition oxygen pressure. The remanent polarization of the film drops with the Bi/Fe ratio. Leakage currents are greatly reduced in Bi-deficient films, resulting from compensation for the oxygen vacancies and suppression of Bi_2O_3 formation. The morphology and ferroelectric domain structures of these films are also very different. The Bi-deficient films typically exhibit small sizes of grains and domains, whereas the stoichiometric films consist of large micrometer size domains. A defect-dipole complex model can be used to explain the different domain structures and the double peaks observed in *C-V* curves.

ACKNOWLEDGMENTS

The authors acknowledge the support from Nanyang Technological University and Ministry of Education of Singapore under Projects No. AcRF RG30/06 and No. ARC 16/08.

*Corresponding author. FAX: (+65) 67909081; jlwang@ntu.edu.sg

[1] J. Wang, J. B. Neaton, H. Zheng, V. Nagarajan, S. B. Ogale, B. Liu, D. Viehland, V. Vaithyanathan, D. G. Schlom, U. V. Waghmare, N. A. Spaldin, K. M. Rabe, M. Wuttig, and R. Ramesh, Science **299**, 1719 (2003).

[2] W. Eerenstein, F. D. Morrison, J. Dho, M. G. Blamire, J. F. Scott, and N. D. Mathur, Science **307**, 1203a (2005).

[3] H. Bea, M. Bibes, S. Fusil, K. Bouzehouane, E. Jacquet, K. Rode, P. Bencok, and A. Barthelemy, Phys. Rev. B **74**, 020101(R) (2006).

[4] J. R. Teague, R. Gerson, and W. J. James, Solid State Commun. **8**, 1073 (1970).

[5] S. V. Kiselev, R. P. Ozerov, and G. S. Zhdanov, Sov. Phys. Dokl. **7**, 742 (1963).

[6] T. Zhao, A. Scholl, F. Zavaliche, K. Lee, M. Barry, A. Doran, M. P. Cruz, Y. H. Chu, C. Ederer, N. A. Spaldin, R. R. Das, D. M. Kim, S. H. Baek, C. B. Eom, and R. Ramesh, Nature Mater. **5**, 823 (2006).

[7] D. Lebeugle, D. Colson, A. Forget, M. Viret, A. M. Bataille, and A. Goukasov, Phys. Rev. Lett. **100**, 227602 (2008).

[8] Y. H. Chu, L. W. Martin, M. B. Holcomb, M. Gajek, S.-J. Han, Q. He, N. Balke, C.-H. Yang, D. Lee, W. Hu, Q. Zhan, P.-L. Yang, A. Fraile-Rodríguez, A. Scholl, S. X. Wang, and R. Ramesh, Nature Mater. **7**, 478 (2008).

[9] F. Kubel and H. Schmid, Acta Crystallogr., Sect. B: Struct. Sci. **46**, 698 (1990).

[10] J. B. Neaton, C. Ederer, U. V. Waghmare, N. A. Spaldin, and K. M. Rabe, Phys. Rev. B **71**, 014113 (2005).

[11] J. F. Li, J. L. Wang, M. Wuttig, R. Ramesh, N. G. Wang, B. Ruette, A. P. Pyatakov, A. K. Zvezdin, and D. Viehland, Appl. Phys. Lett. **84**, 5261 (2004).

[12] M. Murakami, S. Fujino, S.-H. Lim, L. G. Salamanca-Riba, M. Wuttig, I. Takeuchi, B. Varughese, H. Sugaya, T. Hasegawa, and S. E. Lofland, Appl. Phys. Lett. **88**, 112505 (2006).

[13] S. H. Lim, M. Murakami, W. L. Sarney, S. Q. Ren, A. Varatharajan, V. Nagarajan, S. Fujino, M. Wuttig, I. Takeuchi, and L. G. Salamanca-Riba, Adv. Funct. Mater. **17**, 2594 (2007).

[14] H. Bea, M. Bibes, A. Barthélémy, K. Bouzehouane, E. Jacquet, A. Khodan, J.-P. Contour, S. Fusil, F. Wyczisk, A. Forget, D. Lebeugle, D. Colson, and M. Viret, Appl. Phys. Lett. **87**, 072508 (2005).

[15] J. F. Ihlefeld, A. Kumar, V. Gopalan, D. G. Schlom, Y. B. Chen, X. Q. Pan, T. Heeg, J. Schubert, X. Ke, P. Schiffer, J. Orenstein, L. W. Martin, Y. H. Chu, and R. Ramesh, Appl. Phys. Lett. **91**, 071922 (2007).

[16] R. L. Holman, Ferroelectrics **14**, 675 (1976).

[17] M. Dawber, K. M. Rabe, and J. F. Scott, Rev. Mod. Phys. **77**, 1083 (2005).

[18] S. Aggarwal and R. Ramesh, Annu. Rev. Mater. Sci. **28**, 463 (1998).

[19] G. E. Pike, W. L. Warren, D. Dimos, B. A. Tuttle, R. Ramesh, J. Lee, V. G. Keramidas, and J. T. Evans, Jr., Appl. Phys. Lett. **66**, 484 (1995).

[20] Q. Tan, J. X. Li, and D. Viehland, Appl. Phys. Lett. **75**, 418 (1999).

[21] S. J. Clark and J. Robertson, Appl. Phys. Lett. **90**, 132903 (2007).

[22] S. T. Zhang, Y. Zhang, M. H. Lu, C. L. Du, Y. F. Chen, Z. G. Liu, Y. Y. Zhu, N. B. Ming, and X. Q. Pan, Appl. Phys. Lett. **88**, 162901 (2006).

[23] G. D. Hu, X. Cheng, W. B. Wu, and C. H. Yang, Appl. Phys. Lett. **91**, 232909 (2007).

[24] S. K. Singh, K. Maruyama, and H. Ishiwara, Appl. Phys. Lett. **91**, 112913 (2007).

[25] B. F. Yu, M. Y. Li, Z. Q. Hu, L. Pei, D. Y. Guo, X. Z. Zhao, and S. X. Dong, Appl. Phys. Lett. **93**, 182909 (2008).

[26] D.-J. Kim, J.-P. Maria, A. I. Kingon, and S. K. Streiffer, J. Appl. Phys. **93**, 5568 (2003).

[27] C. W. Bark, S. Ryu, Y. M. Koo, H. M. Jang, and H. S. Youn, Appl. Phys. Lett. **90**, 022902 (2007).

[28] G. Catalan, H. Bea, S. Fusil, M. Bibes, P. Paruch, A. Barthelemy, and J. F. Scott, Phys. Rev. Lett. **100**, 027602 (2008).

[29] J. Seidel, L. W. Martin, Q. He, Q. Zhan, Y.-H. Chu, A. Rother, M. E. Hawkridge, P. Maksymovych, P. Yu, M. Gajek, N. Balke, S. V. Kalinin, S. Gemming, F. Wang, G. Catalan, J. F. Scott, N. A. Spaldin, J. Orenstein, and R. Ramesh, Nature Mater. **8**, 229 (2009).